AGU PUBLICATIONS

JGR

Journal of Geophysical Research: Atmospheres

RESEARCH ARTICLE
10.1002/2015JD023914

Summertime surface O_3 behavior and deposition to tundra in the Alaskan Arctic

Brie Van Dam[1,2], Detlev Helmig[1], Paul V. Doskey[3,4], and Samuel J. Oltmans[5,6]

[1]Institute of Arctic and Alpine Research, University of Colorado Boulder, Boulder, Colorado, USA, [2]Now at the Institute of Arctic Biology, University of Alaska Fairbanks, Fairbanks, Alaska, USA, [3]School of Forest Resources and Environmental Science, Michigan Technological University, Houghton, Alaska, USA, [4]Atmospheric Sciences Program, Michigan Technological University, Houghton, Michigan, USA, [5]CIRES, University of Colorado Boulder, Boulder, Colorado, USA, [6]ESRL Global Monitoring Division, NOAA, Boulder, Colorado, USA

Key Points:
- A diurnal ozone cycle with mean magnitude of 13 ppbv developed at Toolik Lake following snowmelt
- Characterized ozone deposition velocity over Arctic tundra
- Ozone deposition velocity demonstrated a diurnal cycle

Supporting Information:
- Supporting Information S1
- Figure S1
- Figure S2
- Figure S3
- Figure S4
- Figure S5
- Figure S6
- Figure S7
- Figure S8
- Figure S9

Correspondence to:
D. Helmig,
detlev.helmig@colorado.edu

Citation:
Van Dam, B., D. Helmig, P. V. Doskey, and S. J. Oltmans (2016), Summertime surface O_3 behavior and deposition to tundra in the Alaskan Arctic, *J. Geophys. Res. Atmos.*, *121*, 8055–8066, doi:10.1002/2015JD023914.

Received 9 JUL 2015
Accepted 16 APR 2016
Accepted article online 23 APR 2016
Published online 7 JUL 2016

Abstract Atmospheric turbulence quantities, boundary layer ozone (O_3) levels, and O_3 deposition to the tundra surface were investigated at Toolik Lake, AK, during the 2011 summer season. Beginning immediately after snowmelt, a diurnal cycle of O_3 in the atmospheric surface layer developed with daytime O_3 maxima, and minima during low-light hours, resulting in a mean amplitude of 13 ppbv. This diurnal O_3 cycle is far larger than observed at other high Arctic locations during the snow-free season. During the snow-free months of June, July, and August, O_3 deposition velocities were ~3 to 5 times faster than during May, when snow covered the ground most of the month. The overall mean O_3 deposition velocity between June and August was 0.10 cm s^{-1}. The month of June had the highest diurnal variation, with a median O_3 deposition velocity of 0.2 cm s^{-1} during the daytime and 0.08 cm s^{-1} during low-light conditions. These values are slightly lower than previously reported summertime deposition velocities in northern latitudes over tundra or fen. O_3 loss during low-light periods was attributed to a combination of surface deposition to the tundra and stable boundary layer conditions. We also hypothesize that emissions of reactive biogenic volatile organic compounds into the shallow boundary layer may contribute to nighttime O_3 loss.

1. Introduction

Levels of ozone (O_3) in the troposphere have more than doubled since preindustrial times due largely to increased emissions of photochemical precursors [*Lelieveld and Dentener*, 2000; *Fusco and Logan*, 2003; *Vingarzan*, 2004; *Lamarque et al.*, 2005; *Oltmans et al.*, 2006]. The chemistry of O_3 is of interest due to its impact on the oxidation capacity of the atmosphere, the role of O_3 as a harmful pollutant, and the contribution of O_3 to greenhouse gas forcing. Important environmental and land surface changes including accelerated warming, sea ice loss, and reductions in snow cover and permafrost extent are occurring in the Arctic [*Lemke et al.*, 2007; *Trenberth et al.*, 2007; *Post et al.*, 2009; *Cavalieri and Parkinson*, 2012]. O_3, a reactive gas, interacts and gets destroyed on surfaces, and the rate of O_3 loss is sensitive to the type of substrate and land cover. Consequently, land surface changes are expected to alter the sink and budget of O_3 in the Arctic. Improving our understanding of O_3-surface interactions is of interest given the importance of O_3 as a vegetation stressor, in atmospheric chemistry and climate, and for improving our representation of loss processes in chemistry climate models. Improved understanding is particularly important for higher accuracy projections of climate feedbacks in the Arctic and lower latitudes.

Quantifying the contribution of sources and sinks of tropospheric O_3 has been a focus of several campaigns over the past few decades [*Gregory et al.*, 1992; *Mauzerall et al.*, 1996; *Wang et al.*, 2003; *Dibb et al.*, 2003; *Stroud et al.*, 2004; *Jacob et al.*, 2010]. In the remote Northern Hemisphere the important source terms include transport (via intrusion of stratospheric air as well as long-range tropospheric transport) and in situ photochemical production [*Gregory et al.*, 1992; *Dibb et al.*, 2003; *Stroud et al.*, 2004]. In situ photochemical loss and deposition at the surface are the primary loss mechanisms [*Gregory et al.*, 1992]. The seasonal cycle of tropospheric O_3 in the Arctic has been shown to display a distinct springtime maximum and summer minimum [*Monks*, 2000; *Helmig et al.*, 2007]. Multiple surface O_3 phenomena have been discovered in the high latitudes that demonstrate the importance of snow photochemistry and snow-atmosphere interactions on atmospheric O_3 chemistry. These include the occurrence of tropospheric O_3 depletion events (ODEs) in the springtime

[*Barrie et al.*, 1988; *Oltmans et al.*, 1989], and production of O_3 in the stable surface layer as documented at the South Pole [*Crawford et al.*, 2001; *Helmig et al.*, 2008].

Research presented here focuses on surface layer O_3 measurements on the North Slope of Alaska in the summertime. Tundra makes up a large portion of the land surface area in the high northern latitudes. There are limited publications that report on O_3 surface fluxes to the snow-free Arctic, particularly over tundra. *Jacob et al.* [1992b] measured mean hourly O_3 deposition velocities (v_d) in southwest AK between July and August 1988 ranging between 0.24 cm s^{-1} during the day and 0.12 cm s^{-1} at night. In northern Finland over a flark fen (composed of open water pools, bare peat, and ridges of drier ground) a weak diurnal cycle in O_3 v_d, with observations between 0.15 and 0.2 cm s^{-1} between night and day, respectively [*Tuovinen et al.*, 1998]. Over a fen in northern Quebec a mean value of 0.17 cm s^{-1} was observed during daytime [*Moore et al.*, 1994]. Past modeling work has shown that incorporating a mechanistic O_3 photochemistry scheme and diurnal representation of the O_3 surface deposition velocity with explicitly calculated stomatal and other resistance can yield up to 10% improvement in model versus observation summertime O_3 dry deposition [*Ganzeveld and Lelieveld*, 1995]. The length of the snow-free season in the Arctic has been observed to be increasing by up to ~9 d $decade^{-1}$ [*Chapin et al.*, 2005]. These changes imply that the strength of the Arctic as an O_3 sink is increasing. In this study we investigate controls on the surface layer O_3 budget in summer by first characterizing the influence of snowmelt on the dynamics of O_3 at an Arctic tundra location. Next, the influence of boundary layer stability and surface deposition as primary controls on the diurnal cycle observed in surface O_3 are examined. Lastly, eddy covariance is used to quantify the magnitude and diurnal cycle of surface O_3 deposition velocities.

2. Measurements

2.1. Site Characterization

Measurements were conducted at the University of Alaska Fairbanks' Institute of Arctic Biology Toolik Field Station (68.6°N, 149.6°W, 720 m above sea level (asl)). Toolik Lake is located in the foothills region of the Brooks Range on the North Slope of Alaska. This region is underlain by continuous permafrost ~200 m deep, with an active layer of soil that thaws annually between 30 cm and 2 m thick [*Hobbie and Kling*, 2014]. Four main terrestrial ecosystem types are present in the Toolik Lake region: tussock tundra, heath, wet sedge tundra, and deciduous shrub stands [*Hobbie and Kling*, 2014]. Aside from Toolik Lake, many smaller lakes, streams, and rivers exist in the region. Measurements described here were made at a 4 m tower at the southern edge of Toolik Lake (south west of the main field station facilities). The tower was in an area of mainly dry heath tundra, with moist tussock tundra comprising much of the extended region to the south and southwest [*Walker and Maier*, 2008]. Figure 1 shows Toolik Lake, the field station (located in the sector designated S1), as well as the location of the measurement tower.

2.2. Ambient Measurements and Surface Turbulence

Atmospheric O_3 and surface turbulence measurements were conducted above the tundra surface during a full year spanning September 2010 to August 2011. In this analysis, we focus on the snow-free period including snowmelt in May through 31 August 2011. A UV photometric O_3 analyzer with an inlet sampling at 4.1 m on the tower, a 3-D sonic anemometer at 3.4 m, and an incoming solar radiation sensor were deployed. A detailed description of these instruments, the tower, sampling methods, and turbulence data processing is included in *Van Dam et al.* [2013]. The O_3 flux measurements are described below. To avoid erroneous sampling of emissions from the field camp facilities, sampling periods from sector S1 were removed during analysis of the chemical data. This removed 10.9% of the data between 25 May and 31 August. A wind rose showing wind speed as a function of the wind direction between 1 June and 31 August is shown in Figure 1 as well. During the summer low wind speeds were prevalent at Toolik Lake, with winds not exceeding 10 m s^{-1}. Winds had two primary directions, either from the south to south-southeast or from the northwest to north. Ambient temperatures in June, July, and August ranged from nighttime lows of −5°C early and late in the season to daytime highs up to 25°C in midsummer [*Van Dam et al.*, 2013].

Surface O_3 data from Barrow, AK, (71.3°N, 156.6°W, 8 m asl) and Tiksi, Russia, (71.6°N, 128.9°E, 7 m asl) were also used. These measurements were collected by the NOAA Earth System Research Laboratory (ESRL) Global Monitoring Division using a Thermo Environmental Instruments (TEI) model 49i UV photometric O_3 analyzer (data available at http://www.esrl.noaa.gov/gmd/dv/data/). Toolik Lake is located ~225 km inland, whereas Barrow and Tiksi are both coastal sites. Additional information on the Tiksi and Barrow observatories can be found at http://www.esrl.noaa.gov/gmd/.

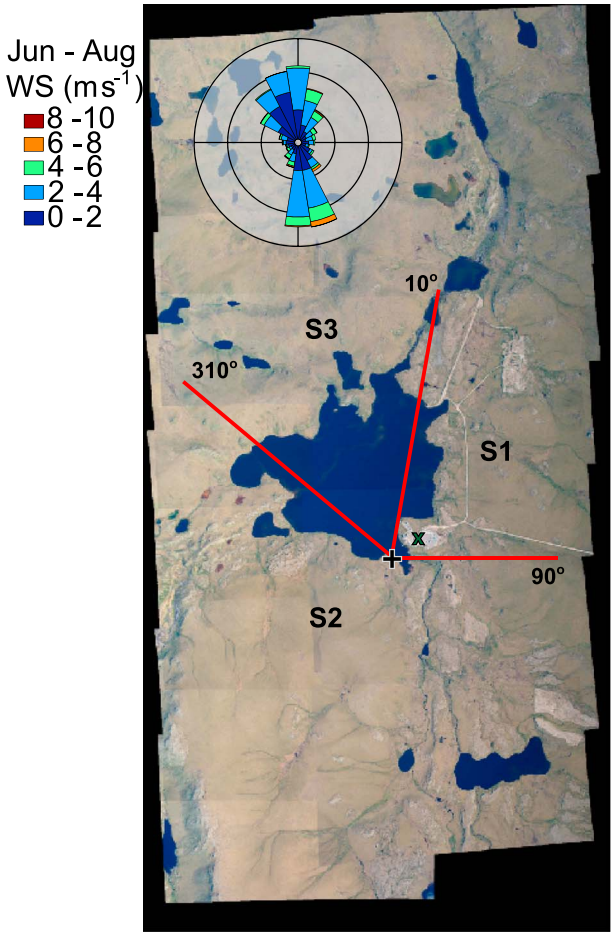

Figure 1. Toolik Lake and surrounding area from *Toolik Field Station Geographical Information Systems and Remote Sensing Team* [2013]. Overlain on the photo is the location of the sampling site (black plus), the location of the field station (cross), and the red lines indicate sectors described in the text. The Toolik Field Station camp facilities can be seen at the southeast side of the lake in S1. The sampling site was approximately 350 m west of the camp facilities. Sector S2 contains a mainly tundra footprint, whereas sector S3 includes Toolik Lake. Data from the 3-D sonic anemometer were implemented to create the wind rose at top left in the figure, showing wind speeds as a function of the wind direction averaged over June through August 2011.

2.3. O_3 Fluxes

The eddy covariance method was used to calculate surface O_3 fluxes (F_{O_3}). The primary components of this measurement method include a 3-D sonic anemometer (referenced in the previous section) and a fast-response chemiluminescence O_3 instrument (FRCI). The FRCI is based in principle on the chemiluminescence reaction of O_3 with nitric oxide (NO). This instrument was developed for highly sensitive eddy covariance O_3 flux determination over the ocean and has been deployed on numerous ship cruises and at Barrow, AK, and is described in detail by *Bariteau et al.* [2010], *Helmig et al.* [2012a, 2012b], and *Boylan et al.* [2014]. More detail on the sonic anemometer and FRCI as it was operated at Toolik Lake, including a comparison with a UV photometric ozone analyzer, is presented in *Van Dam et al.* [2013]. At Toolik Lake, the FRCI was used with a 35 m sampling line with an inner diameter of 0.64 cm and outer diameter of 0.95 cm. A perfluoroalkoxy filter holder (Savillex Corp., Minnetonka, MN) housed a Teflon membrane filter (5 μm, Millipore, Billerica, MA) at the inlet, which was colocated with the 3-D sonic anemometer at 3.4 m above the tundra surface. The line and filter were conditioned by purging with approximately 300 ppbv of O_3 at a flow rate of 3 L min^{-1} for 24 h prior to use. The flow rate in the purge line was controlled to 8 L min^{-1} using a mass flow controller, and the FRCI sample flow rate was controlled at 1.5 L min^{-1}. The instrument sensitivity was approximately 2360 counts s^{-1} ppbv^{-1}. The time delay between the turbulence measurements and the O_3 signal acquisition (delayed due to transport time of air between the inlet and the FRCI reaction chamber) was determined on a regular basis using a puff

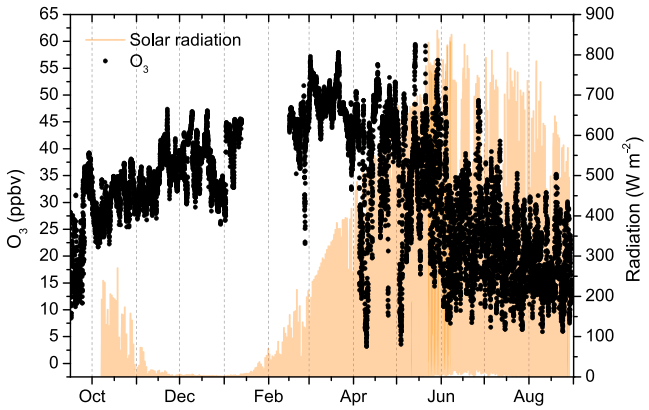

Figure 2. Annual cycle of O_3 measured at 4.1 m above the surface (black dots, left axis) and incoming solar radiation (1 min, orange line, right axis) at Toolik Lake. Both O_3 and solar radiation are 30 min mean values. The measurement period spans September 2010 through August 2011, although the solar radiation sensor was not installed until the beginning of October 2010.

system [*Bariteau et al.*, 2010]. The average lag time during the summer period was 6 s. Fluxes were calculated in 30 min increments with units of $\mu g\ s^{-1}\ m^{-2}$ and are converted to deposition velocities ($v_d = -F_{O_3}/[O_3]$) to remove the dependence on the O_3 mixing ratio. Deposition velocities are reported in $cm\ s^{-1}$, with positive values indicating a downward flux to the surface (deposition).

In addition to the wind direction filter mentioned above, data were filtered for low wind speeds (less than $0.5\ m\ s^{-1}$) due to the difficulty in determining the magnitude of the streamwise wind accurately at low wind speeds. The determination of O_3 fluxes relies on the assumption of a constant flux layer (meaning the variation in vertical turbulent fluxes with height is less than 10% of the magnitude). The Monin-Obukhov length ratio, zL^{-1}, was used to evaluate stability conditions, where z is the measurement height, and L is the Monin-Obukhov length defined as follows:

$$L = \frac{-u_*^3 T_0}{kgH_s} \quad (1)$$

In this equation, T_0 is the temperature, u_* is the friction velocity, k is the von Karman constant, g is gravitational acceleration, and H_s is the sensible heat flux. Periods when zL^{-1} was greater than 0.2 were filtered, as this indicates conditions are too stable for a constant flux layer to exist [*Sorbjan and Grachev*, 2010]. Another requirement for O_3 flux calculations is the stationarity of the mean O_3 mixing ratio; therefore, data were filtered for periods when the standard deviation of 1 min O_3 readings during the 30 min period exceeded 3 ppbv [*Bariteau et al.*, 2010]. In total, all of the filters accounted for the removal of 46% of the data between May and August 2011.

3. Results and Discussion

3.1. Year-Round Variation in O_3 at Toolik Lake

To provide context for the summertime measurements, the annual cycle of ambient O_3 mixing ratios is shown in Figure 2. Incoming solar radiation levels at Toolik Lake vary from less than 50 W m^{-2} during the winter months to greater than 750 W m^{-2} during daytime in summer. Surface layer O_3 values show a generally increasing trend starting in the beginning of the measurement period in September and reaching maximum values of 55–59 ppbv in early spring (March–May). The influence of ODEs is observed beginning in April as investigated in detail by *Van Dam et al.* [2013]. The summertime months of June, July, and August are characterized by the lowest mean values for the seasonal record, aside from measured ODEs. Generally, higher O_3 levels occur during winter and early spring when incoming solar radiation levels (and therefore photochemical loss processes) are low. The trend in this seasonal cycle, with early springtime maximum and summer minimum O_3 levels, is characteristic of many documented Arctic locations [*Oltmans et al.*, 1996; *Monks*, 2000; *Helmig et al.*, 2007]. Strikingly for an Arctic site, however, the summertime O_3 values vary from less than 10 ppbv (similar magnitude as observations during springtime ODEs) to greater than 35 ppbv. Upon closer inspection it can be seen that this variability is actually a marked diurnal cycle in O_3 mixing ratios observed at Toolik Lake beginning in late May. This feature is considered in detail in the following sections.

3.2. Diurnal O_3 Dynamics

3.2.1. Changes in Surface O_3 Behavior After Snowmelt

The initiation of the diurnal surface O_3 cycle in spring is described in Figure 3. Due to the variable topography at Toolik Lake, snow depth is not homogeneous in the area surrounding the measurement site. These

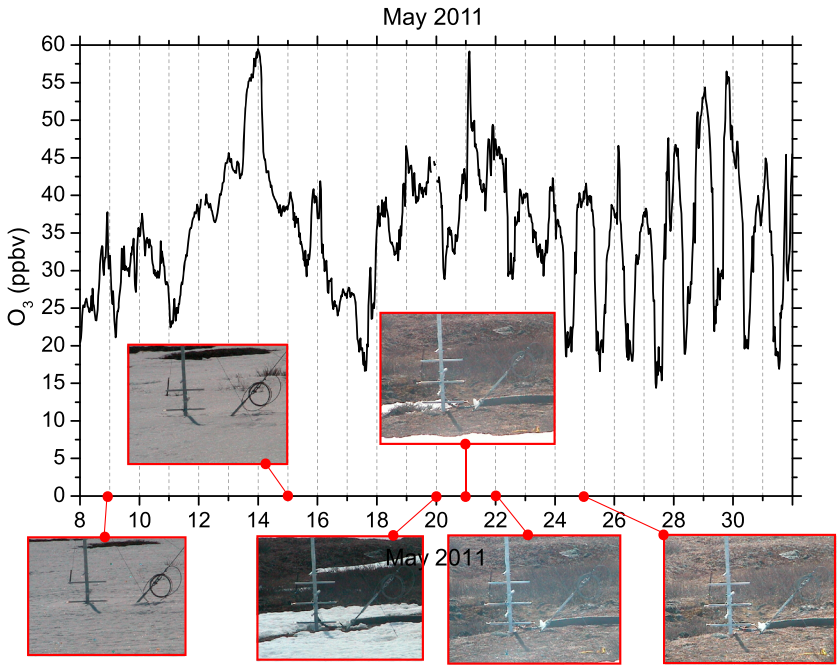

Figure 3. Thirty minute mean O_3 measured at 4.1 m above the surface for the period 8–31 May 2011. Overlain on this plot are images from a webcam mounted on the instrument building. The webcam monitored snow extent near a snow interstitial air sampling tower, which was adjacent to the tower that held the O_3 sampling inlet. The red lines and dots indicate the day the photo was taken along the time axis of the figure. All photos were taken at ~12:00 AKST. Small topographical variations significantly influence snow depth and extent around Toolik Lake, but the site was essentially snow free on 22 May.

images show the snow tower site becoming snow free between 20 and 22 May. Shortly after the time rapid snowmelt began on 20 May, a diurnal cycle in surface O_3 developed with nighttime minima occurring at 02:00–06:00 Alaska Standard Time (AKST), and daytime maxima occurring between 14:00 and 19:00 AKST. An amplitude on the order of 10–15 ppbv was measured initially near the snow tower, increasing to a daily value of 20 ppbv by 24 May (Figure 4). Snowmelt in the surrounding tundra continued through the month, and the field station did not report the surrounding tundra as 100% snow free until 15 June [*Environmental Data Center Team*, 2013]. By the end of the month, there was on average a 20–30 ppbv difference between nighttime and daytime O_3 values. The amplitude of the diurnal cycle in O_3 shows a generally decreasing trend between 1 June and 31 August. A linear regression analysis of the data indicates that the amplitude of the diurnal O_3 cycle diminished in magnitude by just over 0.1 ppbv d^{-1} on average; this amounts to approximately 10 ppbv over the 3 month summer period.

Figure 4. Change in the amplitude of the diurnal cycle of surface O_3 from 1 June to 31 August 2011. The amplitude was calculated by subtracting the minimum 10 min mean value from the maximum 10 min mean value for each 24 h period. Black dots show the calculated amplitude, while the red line shows a five-point running mean of the data.

3.2.2. Comparison of Surface O_3 in Summer at Snow-Free Arctic Sites

A comparison with two other Arctic locations with available surface O_3 records and snow-free conditions during July 2011 (Barrow and Tiksi) illustrates the unique conditions at Toolik Lake. Figure 5 shows the median diurnal cycle in surface O_3 from each of these three sites in July 2011. The

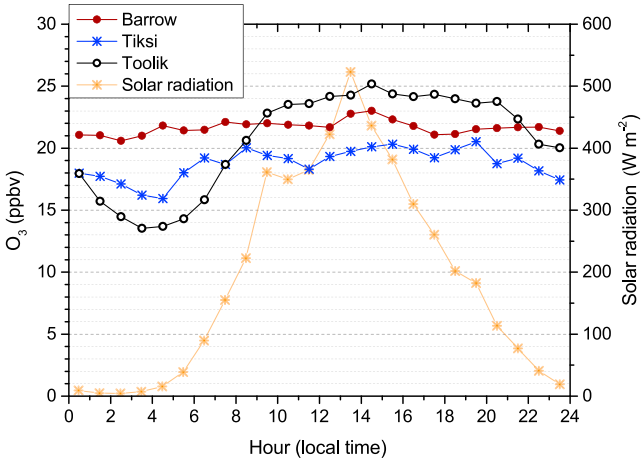

Figure 5. Comparison of the summertime (1–31 July) median surface O_3 diurnal cycle between three Arctic locations: Toolik Lake (open black circles), Tiksi (blue stars), and Barrow (dark red dots). Average diurnal cycles were calculated from the median O_3 value over the month for each hour of the day. The average July incoming solar radiation (orange stars) data from Toolik Lake are shown as well.

median hourly values of incoming solar radiation as measured at Toolik Lake during the same time period are shown for reference, although solar radiation conditions were different at each of these sites due to their varying locations. With a 12 ppbv difference between the daily maximum and minimum averaged over July, Toolik Lake showed the largest median diurnal cycle amplitude. The shape of the diurnal cycle at Toolik Lake is distinct from the other sites, with the lowest daily value of 13.5 ppbv (the median value measured at 03:00 AKST). Tiksi and Barrow show very small changes in O_3 levels throughout the day. The diurnal cycle amplitude at Barrow has been investigated previously and found to exhibit an amplitude during June of approximately 1.0–1.2 ppbv [*Oltmans*, 1981; *Helmig et al.*, 2007]. The amplitude at Tiksi during June 2011 was on the order of 4.5 ppbv.

The only other evidence of a diurnal O_3 cycle over tundra, with a magnitude approximately half of what is reported here, is described in *Jacob et al.* [1992a]. That study was part of the Arctic Boundary Layer Expedition (ABLE 3A), where surface O_3 mixing ratios and deposition velocities were measured near Bethel in southwest Alaska (61.08°N, 162.04°W) in 1988. That measurement location is similar to Toolik Lake in that it is composed of flat terrain ranging from dry upland to wet meadow tundra, interspersed with small lakes. Over a 30 day measurement period spanning July–August *Jacob et al.* [1992a] measured an average range of surface O_3 values between 17 ppbv in the early morning hours and 25 ppbv in the late afternoon. Measurements at other northern latitude sites besides those discussed here have shown much smaller diurnal cycle amplitudes [*Tuovinen et al.*, 1998]. Nitrogen oxides (NO_x, NO + NO_2) have been measured at several Arctic locations. *Honrath and Jaffe* [1992] measured NO at less than 10 pptv during most periods at Barrow, AK, and *Bakwin et al.* [1992] measured NO_x levels less than 20 pptv during the ABLE 3A experiment. These levels are too low for O_3 production. Therefore, the diurnal O_3 cycle is most likely driven by other factors discussed below.

3.2.3. Atmospheric Transport and Surface O_3

The relationship between O_3 and atmospheric transport was investigated using observed O_3 mixing ratios, and wind speed and wind direction derived from the sonic anemometer measurements. As mentioned above, wind speeds were frequently lower at night (on average <2 m s^{-1}, Figure S1 in the supporting information), with wind directions often considered variable due to low wind. The hourly wind direction data (Figures S2–S6 in the supporting information) show that the site experiences diurnally changing flow regimes, which could be considered upslope-downslope flow patterns due to local topography. During daytime, for 5–9 h (April–August) flows are primarily from the northwest to north, which is the direction of slightly downsloping terrain (supporting information Figure S7). During late afternoon to late morning winds from the south (direction of the Brooks Range 20 km from the site) were dominant. Other previous research has shown diurnally changing O_3 mixing ratios associated with upslope/downslope flow occurrence at or near mountain slopes. For instance, at Mauna Loa Observatory (MLO), transport is primarily upslope during daytime, driven by surface heating of the black mountain slopes [*Mendoca*, 1969], and downslope during the nighttime due to surface cooling. Surface O_3 at MLO shows a distinct diurnal cycle, with lower O_3 observed in upsloping air during late morning to late evening hours, and O_3 increasing steadily throughout the night as downslope flow replaces the daytime surface layer [*Oltmans*, 1981]. Higher O_3 in downslope airflow reflects the elevation gradient of O_3, as O_3 generally increases with altitude. However, O_3 behavior at Toolik Lake is opposite to this mountain flow regime. In the data presented here, the highest diurnal O_3 levels are observed in upslope flow during the daytime, whereas at night, with southerly winds and downslope flows, O_3 is at a minimum. Figures S8 and S9 in the supporting information show that low O_3 levels were seen both in northerly

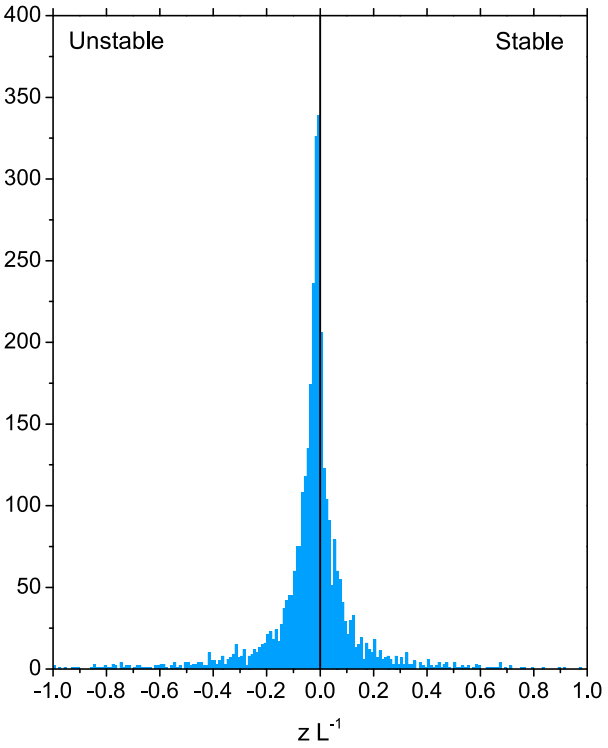

Figure 6. Histogram of zL^{-1} for June–August (30 min averaged data). Negative values indicate unstable conditions, and positive values suggest stable conditions.

and southerly wind conditions, with southerly winds associated with a slightly higher abundance of low O_3 occurrences. These analyses discount the hypothesis that wind direction is a driver of O_3 levels at the site, as does a similar plot describing springtime O_3 levels in *Van Dam et al.* [2013].

3.2.4. Atmospheric Turbulence and Surface O_3

A histogram showing the distribution of zL^{-1} measured June through August at Toolik Lake is shown in Figure 6. During the summer period, stable conditions (positive zL^{-1}) were measured approximately 23% of the time. Unstable conditions (negative zL^{-1}) were measured 50% of the period; no value for zL^{-1} was obtained for 27% due to either instrumental issues or one of the quality control filters described above. Figure 7 shows these data plotted as median hourly values over the June through August period. Values of the stability parameter were negative, indicating unstable atmospheric conditions, during sunlit hours. Conditions transitioned to near neutral and stable during low-light hours, from approximately 21:00–06:00 AKST. This is indicative of a stable and stratified boundary layer during nighttime and coincides with the time when O_3 levels were seen to decrease significantly.

To investigate the relationship between O_3 levels and atmospheric stability in more detail, two 6 day periods in (a) June and (b) August were investigated (Figure 8). The amplitude of the diurnal O_3 cycle was approximately 20 ppbv in the June period, and slightly less at approximately 15 ppbv during the August period. A clear relationship can be distinguished in Figure 8 between generally stable atmospheric conditions and the periods when low O_3 values were observed. It is also notable that the duration of unstable conditions with higher O_3 values is longer in early June than in August. To quantify the relationship between O_3 levels and boundary layer stability, O_3 data were divided into stable and unstable conditions determined by zL^{-1} (Figure 9). O_3 data recorded during unstable conditions had higher mean and median values (22 ppbv and 21 ppbv, respectively) than during stable conditions (19 ppbv and 17 ppbv, respectively). There was a statistically significant difference in the mean O_3 mixing ratios during stable conditions and unstable conditions, as determined by a two-sample t test with $t(3157) = 12.2, p < 0.001$. No statistically significant relationship existed between O_3 mixing ratios and other parameters useful in characterizing boundary layer conditions such as friction velocity and the sensible heat flux.

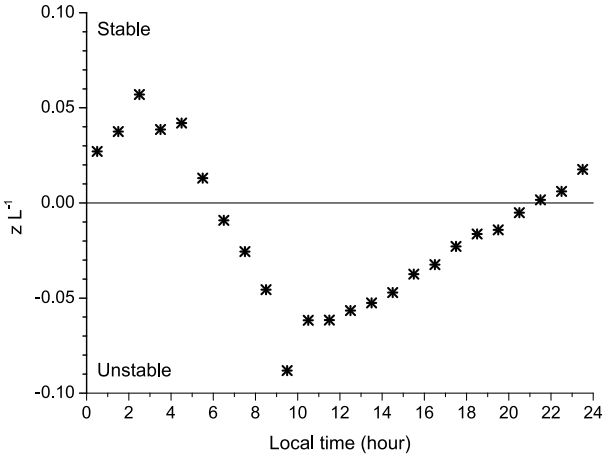

Figure 7. Average summertime diurnal cycle of zL^{-1} at Toolik Lake, calculated by taking the median value of the June–August data over each hour of the day. Conditions were generally stable between 22:00 and 06:00 AKST, and generally unstable during 07:00–20:00 AKST.

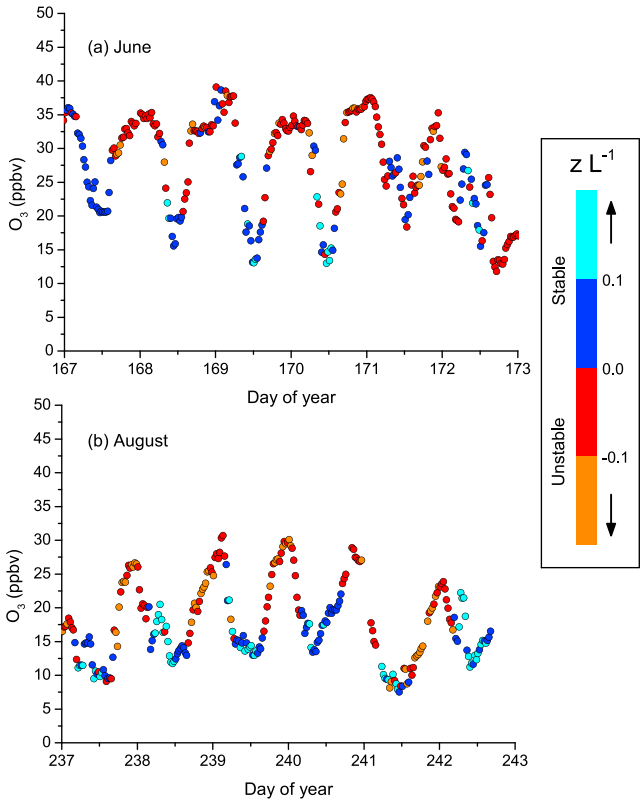

Figure 8. Time series of surface O_3 data for selected periods in (a) June and (b) August. Data are color coded by the value of zL^{-1} in order to associate O_3 levels with stability conditions. The dark and light blue colors indicate varying degrees of weakly stable to stable conditions, and the red hued colors indicate periods when conditions were neutral to unstable.

The above results suggest that the occurrence of a stably stratified atmosphere during low-light hours is an important control on O_3 values at this location. It has been shown previously that significant O_3 reductions at night in rural areas can be observed as a result of surface deposition during stable atmospheric conditions [*Johansson and Janson*, 1993; *Wesely and Hicks*, 2000]. Surface deposition to the tundra is investigated below.

3.3. Characterization of Surface O_3 Deposition Velocities

O_3 deposition velocities were calculated for the months of May, June, July, and August 2011. Implementing the quality control filters described in the measurements section left 54% of O_3 v_d measurements remaining. The distribution of the 30 min data is shown as a histogram in Figure 10a and also displayed using a box chart in Figure 10b. The box chart shows that the central 50% of the data was spread between 0.01 and 0.15 cm s^{-1}, and the range of the 10th to 90th percentile of the v_d values in June to August span ~−0.1 to 0.4 cm s^{-1}. The mean O_3 v_d value was 0.1 cm s^{-1}. Based on the hourly median values, the amplitude of the diurnal cycle in v_d was largest in June with a value of 0.12 cm s^{-1} (Figure 11). During this period of maximum amplitude in June there was a statistically significant difference between primarily light and low-light periods in deposition velocities, using a two-sample *t* test with $t(929) = 3.4$, $p < 0.001$. The mean value during primarily light conditions (10:00–22:59 AKST) was 0.14 cm s^{-1}, and the mean value during primarily low-light conditions (23:00–09:59 AKST) was 0.08 cm s^{-1}. The hourly averaged diurnal cycle amplitude of 0.12 cm s^{-1} in June compares with 0.03 cm s^{-1} in May, 0.10 cm s^{-1} in July, and 0.08 cm s^{-1} in August. Figure 11 also demonstrates two other points: (1) an increase in the magnitude of O_3 v_d moving from May, when the ground was still snow covered for most of the month (Figure 2), to snow-free conditions during June–August, and (2) diurnal minima in surface O_3 coincide with minima in O_3 v_d, occurring between 02:00 and 06:00 AKST. These results suggest that surface deposition to the tundra is an important factor contributing to the diurnal cycle in surface O_3 at Toolik Lake, yet the relatively weak loss of O_3 to the surface at night indicates that other processes may contribute to the O_3 sink during low-light hours as discussed in section 3.4.

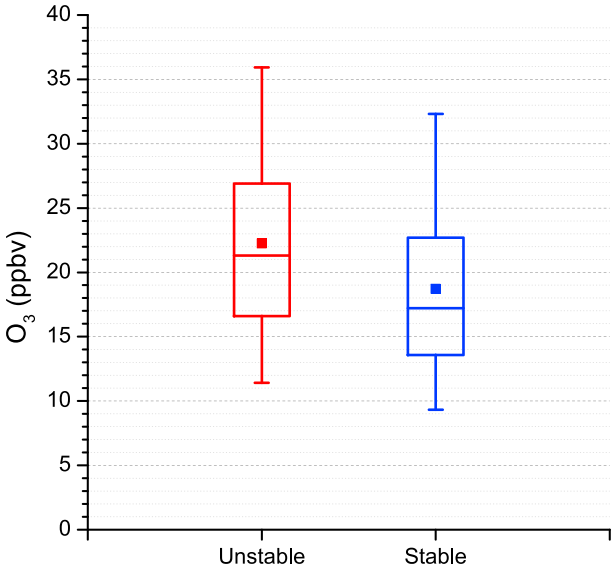

Figure 9. Box whisker charts of O_3 during unstable (red) and stable (blue) conditions defined by the value of zL^{-1} during June–August. Filled squares indicate the mean, the central line in the box indicates the median, and the upper/lower box limit indicates 25th and 75th percentiles. Whiskers show the 5th and 95th percentile of the data.

O_3 v_d to water surfaces, including fresh water and ocean, are known to be small compared to land [*Galbally and Roy*, 1980; *Wesely et al.*, 1981; *Wesely and Hicks*, 2000; *Bariteau et al.*, 2010; *Helmig et al.*, 2012b]. The measurement site sat on the southern shore of Toolik Lake, a 150 ha body of water; therefore, the possible influence of the lake on observed O_3 deposition velocities is investigated. In the deposition velocity measurements detailed above, all wind directions aside from sector S1 (shown in Figure 1) were included in the calculations. The measurement periods were further broken apart into sector S2 (composed of largely dry or moist tussock tundra dotted with small lakes) and sector S3 (containing most of Toolik Lake). The mean v_d from S2 was 0.12 cm s^{-1}, and the mean v_d from S3 was 0.09 cm s^{-1}. A *t* test determined that the difference in the means of the S2 and S3 data sets were statistically significant at the 0.15 level ($t(980) = 1.55, p = 0.12$). This result indicates that calculated deposition velocities when the sampled air mass had traveled over the lake were likely lower than for tundra alone, although the determined significance level suggests that there is ~15% chance that the conclusion of different mean values is in error.

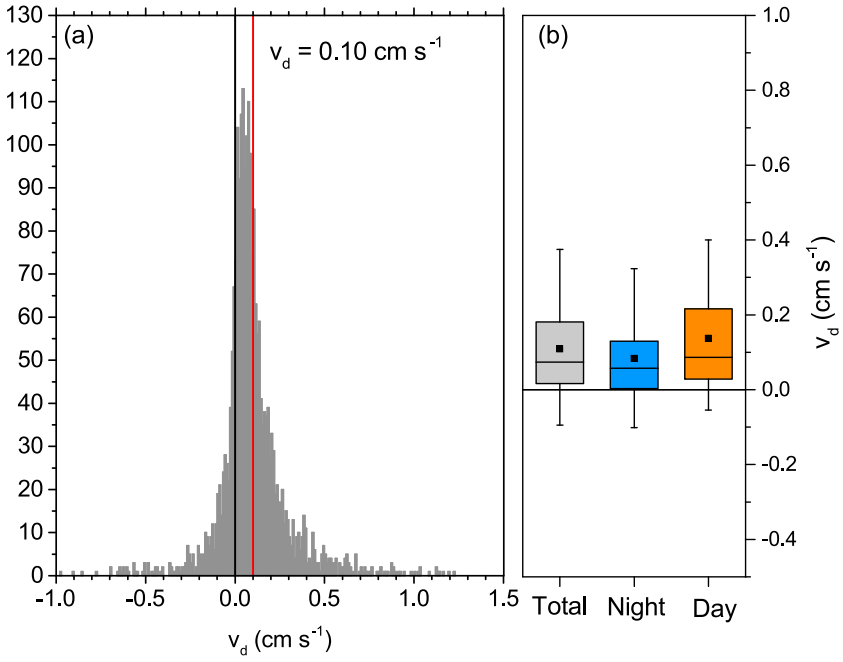

Figure 10. (a) Histogram and (b) box charts of all the 30 min averaged v_d during June to August 2011 (grey box), only data for a primarily light period (10:00–22:59 AKST, orange box), and only data for a primarily low-light period (23:00–09:59 AKST, blue box). The mean value of v_d during this period was 0.11 cm s^{-1}, as indicated by the red line in the histogram. The box chart format in Figure 10b is the same as described in the Figure 9 caption.

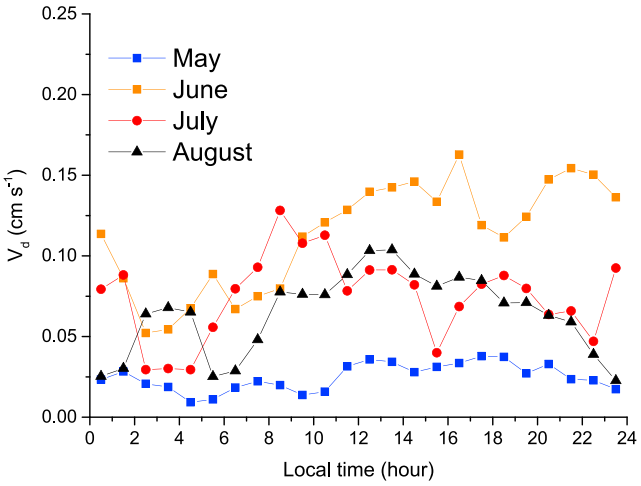

Figure 11. Median value of v_d calculated over each hour for the months of May–August.

3.4. Biogenic Volatile Organic Compounds as O_3 Sink

Diurnal cycles in O_3 at Toolik Lake were not replicated in a modeling experiment using Goddard Earth Observing System-Chem with observed O_3 deposition velocities and stability conditions, which indicates the presence of an O_3 sink that currently is not considered in the model (D. Millet and L. Hu, unpublished data, 2015). A hypothesis that requires further investigation is the possible removal of O_3 by reaction with biogenic volatile organic compound (BVOC) emissions in the shallow surface layer that develops during the night. A number of recent studies have shown unexpectedly high BVOC emissions from tundra vegetation [*Hakola et al.*, 2006; *Tiiva et al.*, 2008; *Potosnak et al.*, 2013; *Rinnan et al.*, 2014]. *Potosnak et al.* [2013] measured leaf-level emission rates of isoprene from *Salix pulchra* and whole system fluxes of isoprene from a moist acidic tussock tundra ecosystem near Toolik Lake. That study found significant emission rates of isoprene and demonstrated, using an atmospheric chemistry box model approach, that in this low NO_x environment the observed isoprene emissions were sufficient to increase the loss rate of O_3 and lead to a 50% reduction in the maximum daily hydroxyl radical (OH) concentration. Emissions of isoprene, monoterpenes, and sesquiterpenes from herbaceous vegetation are sensitive to temperature and light [*Kesselmeier and Staudt*, 1999]. While nighttime irradiance is significantly lower at night near Toolik Lake (Figure 2), nighttime temperatures and residual light levels during July might still be sufficiently high to sustain BVOC emissions. Reaction of isoprene with O_3 is too slow to influence mixing ratios of O_3 on a diurnal scale. However, reaction of many monoterpenes and sesquiterpenes with O_3 are < 6 h and therefore might be fast enough to remove O_3 at night. Vertical mixing is suppressed during low-light hours at Toolik Lake, so accumulation of BVOCs near the surface is expected even for low emission rates. A conclusive evaluation of the influence of BVOC chemistry on O_3 fluxes is not possible with currently available BVOC observations; a more comprehensive characterization of BVOC emissions at Toolik Lake is required to further address this question.

4. Summary and Conclusion

This study reports on unique behavior in surface O_3 over Arctic tundra at Toolik Lake. Following snowmelt, a diurnal cycle of near-surface O_3 in the atmosphere developed with a mean amplitude of 13 ppbv. This is larger than observations from other high Arctic locations during the snow-free season. The diurnal O_3 cycle was primarily driven by O_3 loss during nighttime, when the atmospheric surface layer exhibited stable conditions.

Summertime O_3 deposition velocities to tundra were shown to have an average value of 0.10 cm s^{-1}. The deposition velocity displayed a diurnal variation that was most pronounced in June, with higher deposition rates during daytime, and lower values during low-light hours. The large difference between O_3 levels during high- and low-light periods is attributed to enhanced mixing with air containing higher O_3 from aloft during the daytime, and uptake of O_3 to the tundra and possible chemical loss in the surface layer promoted by stably stratified conditions during low-light hours. However, it is hypothesized that the reaction of O_3 with BVOCs may be important. Predictions from *Potosnak et al.* [2013] indicate that isoprene emissions from Arctic ecosystems will increase in the future as a result of global climate change, with potential important impacts on the O_3 budget. Further research is necessary to determine the intricate role of fast-reacting BVOC emissions on the behavior of O_3 in the Arctic boundary layer.

O_3 deposition velocities to the snow-covered ground in the Arctic reported in the literature are on the order of a factor of 5 lower than that reported to snow-free Arctic tundra. For instance, for snow covering the glacial ice sheet at Summit Station, Greenland, *Helmig et al.* [2009] reported a diurnal cycle of the O_3 surface exchange,

falling within a range of −0.05 to 0.07 cm s^{-1}. At Summit, the surface uptake of O_3 was modulated by photochemical processes in the surface snowpack. This resulted in higher uptake rates during midday to afternoon hours and a seasonal dependence, with springtime O_3 surface uptake rates of ≤0.01 cm s^{-1}, a factor of 3–4 smaller than average summer values. We found similar behavior in the diurnal and seasonal changes of O_3 deposition, and in the O_3 v_d increasing approximately 3–5 times during the transition period from snow cover to snow free. The observations of larger O_3 deposition to the tundra during snow-free compared with snow-covered times imply that the current trend of a lengthening snow-free season would lead to an increase in the surface O_3 sink in the Arctic O_3 budget.

Acknowledgments
This research was funded by the National Science Foundation Office of Polar Programs grant NSF-OPP-07-1399 and the NSF NWT LTER program. The ambient air ozone data and meteorological data from the Toolik Lake experiment are available through ACADIS and the Tropospheric Ozone Assessment Report (TOAR) database at https://join.fz-juelich.de/accounts/login/. Surface ozone data from Barrow, AK, and Tiksi, Russia, were collected by the NOAA/ESRL Global Monitoring Division and are available at http://www.esrl.noaa.gov/gmd/dv/data/. The authors would like to thank CH2MHill Polar Services for logistical support and the Toolik Field Station staff for assistance with the measurements. J. Hueber, B. Seok, and P. Boylan from INSTAAR at the University of Colorado and M. Dziobak, C. Toro, and L. Kramer from Michigan Technological University provided assistance with the field project. Snow cover estimates and wind direction data used for comparison were provided by the Toolik Field Station Environmental Data Center (available at http://toolik.alaska.edu/edc), which is supported by the National Science Foundation grant NSF-1048361.

References

Bakwin, P. S., S. C. Wofsy, S. M. Fan, and D. R. Fitzjarrald (1992), Measurements of NO_x and NO_y concentrations and fluxes over Arctic tundra, *J. Geophys. Res.*, *97*(D15), 16,545–16,557.
Bariteau, L., D. Helmig, C. W. Fairall, J. E. Hare, J. Hueber, and E. K. Lang (2010), Determination of oceanic ozone deposition by ship-borne eddy covariance flux measurements, *Atmos. Meas. Tech.*, *3*(2), 441–455.
Barrie, L. A., J. W. Bottenheim, R. C. Schnell, P. J. Crutzen, and R. A. Rasmussen (1988), Ozone destruction and photochemical reactions at polar sunrise in the lower Arctic atmosphere, *Nature*, *334*(6178), 138–141.
Boylan, P., D. Helmig, and J. H. Park (2014), Characterization and mitigation of water vapor effects in the measurement of ozone by chemiluminescence with nitric oxide, *Atmos. Meas. Tech.*, *7*, 1231–1244.
Cavalieri, D., and C. Parkinson (2012), Arctic sea ice variability and trends, *Cryosphere*, *6*, 881–889.
Chapin, F. S., et al. (2005), Role of land-surface changes in Arctic summer warming, *Science*, *310*(5748), 657–660.
Crawford, J. H., et al. (2001), Evidence for photochemical production of ozone at the South Pole surface, *Geophys. Res. Lett.*, *28*(19), 3641–3644.
Dibb, J. E., R. W. Talbot, E. Scheuer, G. Seid, L. Debell, B. Lefer, and B. Ridley (2003), Stratospheric influence on the northern North American free troposphere during TOPSE: ^{7}Be as a stratospheric tracer, *J. Geophys. Res.*, *108*(D4), 8363, doi:10.1029/2001JD001347.
Environmental Data Center Team (2013), *Toolik Field Station Naturalist Journal*, Inst. of Arct. Biol., Univ. of Alaska Fairbanks, Fairbanks, Alaska. [Available at http://toolik.alaska.edu/edc/journal/.]
Fusco, A. C., and J. A. Logan (2003), Analysis of 1970–1995 trends in tropospheric ozone at Northern Hemisphere midlatitudes with the GEOS-CHEM model, *J. Geophys. Res.*, *108*(D15), 4449, doi:10.1029/2002JD002742.
Galbally, I. E., and C. R. Roy (1980), Destruction of ozone at the Earth surface, *Q. J. R. Meteorol. Soc.*, *106*(449), 599–620.
Ganzeveld, L., and J. Lelieveld (1995), Dry deposition parameterization in a chemistry general-circulation model and its influence on the distribution of reactive trace gases, *J. Geophys. Res.*, *100*(D10), 20,999–21,012.
Gregory, G. L., B. E. Anderson, L. S. Warren, E. V. Browell, D. R. Bagwell, and C. H. Hudgins (1992), Tropospheric ozone and aerosol observations—The Alaskan Arctic, *J. Geophys. Res.*, *97*(D15), 16,45–16,471.
Hakola, H., H. Hellen, and T. Laurila (2006), Ten years of light hydrocarbons concentration measurements in background air in Finland, *Atmos. Environ.*, *40*(19), 3621–3630.
Helmig, D., S. J. Oltmans, D. Carlson, J. F. Lamarque, A. Jones, C. Labuschagne, K. Anlauf, and K. Hayden (2007), A review of surface ozone in the polar regions, *Atmos. Environ.*, *41*(24), 5138–5161.
Helmig, D., B. Johnson, S. J. Oltmans, W. Neff, F. Eisele, and D. D. Davis (2008), Elevated ozone in the boundary layer at South Pole, *Atmos. Environ.*, *42*(12), 2788–2803.
Helmig, D., L. D. Cohen, F. Bocquet, S. Oltmans, A. Grachev, and W. Neff (2009), Spring and summertime diurnal surface ozone fluxes over the polar snow at Summit, Greenland, *Geophys. Res. Lett.*, *36*, L08809, doi:10.1029/2008GL036549.
Helmig, D., et al. (2012a), Ozone dynamics and snow-atmosphere exchanges during ozone depletion events at Barrow, Alaska, *J. Geophys. Res.*, *117*, D20303, doi:10.1029/2012JD017531.
Helmig, D., E. K. Lang, L. Bariteau, P. Boylan, C. W. Fairall, L. Ganzeveld, J. E. Hare, J. Hueber, and M. Pallandt (2012b), Atmosphere-ocean ozone fluxes during the TEXAQS 2006, STRATUS 2006, GOMECC 2007, GASEX 2008, and AMMA 2008 cruises, *J. Geophys. Res.*, *117*, D04305, doi:10.1029/2011JD015955.
Hobbie, J. E., and G. W. Kling (2014), *Alaska's Changing Arctic: Ecological Consequences for Tundra, Streams, and Lakes*, vol. 1, Oxford Univ. Press, Oxford, New York.
Honrath, R. E., and D. A. Jaffe (1992), The seasonal cycle of nitrogen oxides in the Arctic troposphere at Barrow, AK, *J. Geophys. Res.*, *97*(D18), 20,615–20,630.
Jacob, D. J., S. M. Fan, S. C. Wofsy, P. A. Spiro, P. S. Bakwin, J. A. Ritter, E. V. Browell, G. L. Gregory, D. R. Fitzjarrald, and K. E. Moore (1992a), Deposition of ozone to tundra, *J. Geophys. Res.*, *97*(D15), 16,473–16,479.
Jacob, D. J., et al. (1992b), Summertime photochemistry of the troposphere at high northern latitudes, *J. Geophys. Res.*, *97*(D15), 16,421–16,431.
Jacob, D. J., et al. (2010), The Arctic research of the composition of the troposphere from aircraft and satellites (ARCTAS) mission: Design, execution, and first results, *Atmos. Chem. Phys.*, *10*(11), 5191–5212.
Johansson, C., and R. W. Janson (1993), Diurnal cycle of ozone and monoterpenes in a coniferous forest—Importance of atmospheric stability, surface exchange, and chemistry, *J. Geophys. Res.*, *98*(D3), 5121–5133.
Kesselmeier, J., and M. Staudt (1999), Biogenic volatile organic compounds (VOC): An overview on emission, physiology and ecology, *J. Atmos. Chem.*, *33*, 23–89.
Lamarque, J. F., P. Hess, L. Emmons, L. Buja, W. Washington, and C. Granier (2005), Tropospheric ozone evolution between 1890 and 1990, *J. Geophys. Res.*, *110*, D08304, doi:10.1029/2004JD005537.
Lelieveld, J., and F. J. Dentener (2000), What controls tropospheric ozone?, *J. Geophys. Res.*, *105*(D3), 3531–3551.
Lemke, P., et al. (2007), *Climate Change 2007: The Physical Science Basis. Contribution of Working Group I to the Fourth Assessment Report of the Intergovernmental Panel on Climate Change*, Cambridge Univ. Press, Cambridge, U. K., and New York.
Mauzerall, D. L., D. J. Jacob, S. M. Fan, J. D. Bradshaw, G. L. Gregory, G. W. Sachse, and D. R. Blake (1996), Origin of tropospheric ozone at remote high northern latitudes in summer, *J. Geophys. Res.*, *101*(D2), 4175–4188.
Mendoca, B. G. (1969), Local wind circulation on the slopes of Mauna Loa, *J. Appl. Meteorol.*, *8*, 531–541.
Monks, P. S. (2000), A review of the observations and origins of the spring ozone maximum, *Atmos. Environ.*, *34*(21), 3545–3561.

Moore, K. E., D. R. Fitzjarrald, S. C. Wofsy, B. C. Daube, J. W. Munger, P. S. Bakwin, and P. Crill (1994), A season of heat, water vapor, total hydrocarbon, and ozone fluxes at a subarctic fen, *J. Geophys. Res.*, *99*(D1), 1937–1952.

Oltmans, S. J. (1981), Surface ozone measurements in clean air, *J. Geophys. Res.*, *86*(C2), 1174–1180.

Oltmans, S. J., R. C. Schnell, P. J. Sheridan, R. E. Peterson, S. M. Li, J. W. Winchester, P. P. Tans, W. T. Sturges, J. D. Kahl, and L. A. Barrie (1989), Seasonal surface ozone and filterable bromine relationship in the high Arctic, *Atmos. Environ.*, *23*(11), 2431–2441.

Oltmans, S. J., D. J. Hofmann, J. A. Lathrop, J. M. Harris, W. D. Komhyr, and D. Kuniyuki (1996), Tropospheric ozone during Mauna Loa Observatory Photochemistry Experiment 2 compared to long-term measurements from surface and ozonesonde observations, *J. Geophys. Res.*, *101*(D9), 14,569–14,580.

Oltmans, S. J., et al. (2006), Long-term changes in tropospheric ozone, *Atmos. Environ.*, *40*(17), 3156–3173.

Post, E., et al. (2009), Ecological dynamics across the Arctic associated with recent climate change, *Science*, *325*(5946), 1355–1358.

Potosnak, M. J., B. M. Baker, L. LeStourgeon, S. M. Disher, K. L. Griffin, M. S. Bret-Harte, and G. Starr (2013), Isoprene emissions from a tundra ecosystem, *Biogeosciences*, *10*(2), 871–889, doi:10.5194/bg-10-871-2013.

Rinnan, R., M. Steinke, T. McGenity, and F. Loreto (2014), Plant volatiles in extreme terrestrial and marine environments, *Plant Cell Environ.*, *37*(8), 1776–1789.

Sorbjan, Z., and A. A. Grachev (2010), An evaluation of the flux-gradient relationship in the stable boundary layer, *Boundary Layer Meteorol.*, *135*(3), 385–405.

Stroud, C., et al. (2004), Photochemistry in the Arctic free troposphere: Ozone budget and its dependence on nitrogen oxides and the production rate of free radicals, *J. Atmos. Chem.*, *47*(2), 107–138.

Tiiva, P., P. Faubert, A. Michelsen, T. Holopainen, J. K. Holopainen, and R. Rinnan (2008), Climatic warming increases isoprene emission from a subarctic heath, *New Phytol.*, *180*(4), 853–863.

Toolik Field Station Geographical Information Systems and Remote Sensing (2013), Inst. of Arct. Biol., Univ. of Alaska Fairbanks, Fairbanks, Alaska. [Available at http://toolik.alaska.edu/gis/.]

Trenberth, K., et al. (2007), *Observations: Surface and Atmospheric Climate Change*, Cambridge Univ. Press, Cambridge, U. K., and New York.

Tuovinen, J. P., M. Aurela, and T. Laurila (1998), Resistances to ozone deposition to a flark fen in the northern aapa mire zone, *J. Geophys. Res.*, *103*(D14), 16,953–16,966.

Van Dam, B., D. Helmig, J. F. Burkhart, D. Obrist, and S. J. Oltmans (2013), Springtime boundary layer O_3 and GEM depletion at Toolik Lake, Alaska, *J. Geophys. Res. Atmos.*, *118*, 3382–3391, doi:10.1002/jgrd.50213.

Vingarzan, R. (2004), A review of surface ozone background levels and trends, *Atmos. Environ.*, *38*(21), 3431–3442.

Walker, D., and H. Maier (2008), *Vegetation in the Vicinity of the Toolik Field Station, Alaska*, Inst. of Arct. Biol., Univ. of Alaska, Fairbanks, Alaska.

Wang, Y. H., et al. (2003), Springtime photochemistry at northern mid and high latitudes, *J. Geophys. Res.*, *108*(D4), 8358, doi:10.1029/2002JD002227.

Wesely, M. L., and B. B. Hicks (2000), A review of the current status of knowledge on dry deposition, *Atmos. Environ.*, *34*(12–14), 2261–2282.

Wesely, M. L., D. R. Cook, and R. M. Williams (1981), Field measurement of small ozone fluxes to snow, wet bare soil, and lake water, *Boundary Layer Meteorol.*, *20*(4), 459–471.